Antiplasmodial Activity of Chemical Constituents of *Artocarpusaltilis* (Parkinson ex F.A.Zorn) Fosberg Stem Bark: An Experimental-cum-Computational Investigation

Seun B. Ogundele*[a,e], Ayodeji O. Oriola[b], Adebola O. Oyedeji[b], Isaac D. Asiyanbola[c], Emmanuel A. Agbebi[a], Olujide O. Olubiyi[d], Felix O. Olorunmola[e], Katherine Babalola[d], Babatunde A. Yusuf[d], Joseph M. Agbedahunsi[e].

[a]Department of Pharmacognosy and Natural Products, College of Pharmacy, Afe Babalola University, Ado-Ekiti, Nigeria.

[b]Department of Chemical and Physical Sciences, Faculty of Natural Sciences, Walter Sisulu University, Mthatha, 5117, South Africa.

[c]Department of Pharmacology, Faculty of Pharmacy, Obafemi Awolowo University, Ile-Ife, 220005, Nigeria.

[d]Department of Pharmaceutical and Medicinal Chemistry, College of Pharmacy, Afe Babalola University, Ado-Ekiti, Nigeria.

[e]Drug Research and Production Unit, Faculty of Pharmacy, Obafemi Awolowo University, Ile-Ife, 220005, Nigeria.

*Corresponding Author

Seun B. Ogundele

Pharmacognosy and Natural Products

College of Pharmacy

Afe Babalola University, Ado-Ekiti, Nigeria

Email:sbogundele@gmail.com; sbogundele@abuad.edu.ng

Tel:+234-7036754820

Abstract

Background

This present study investigated the antiplasmodial activity of crude extract, and dichloromethane fraction of *Artocarpus altilis*stem bark and isolated some chemical constituents present in the dichloromethane fraction of the crude extract.

Methods

Stem barks of *A. altilis* wereextracted by maceration with 80% aqueous ethanol at ambient temperature. The dichloromethane fraction was repeatedly fractionated and subsequently purified by chromatographic methods using silica gel 60 (230-400 mesh size) and Sephadex LH-20 columns to afford Compounds **1, 2,** and**3** which were characterised by analysis of their ^{1}D-NMR, ^{2}D-NMR, and HRESIMS spectra data. Antiplasmodial activity of crude extract, and dichloromethane fraction was evaluated using the 4-day chemosuppresive, prophylactic, and curative assays respectively, while antiplasmodial activity of Compound **3** was tested using the 4-day chemosuppresive assay. To rationalize the possible mechanistic basis of the observed antiplasmodial activity, Compounds **1**, **2**, and **3**, were screened against 54 macromolecular targets relevant to the establishment of the malaria infection.

Results

Two steroidal triterpenoids: Stigmasterol **1**, 24(25)-Dihydronorstigmasterol (Artophytosterol), **2**, and a flavonoid, Artocarpentanol, **3** were identified by spectroscopic analysis. The crude extract, dichloromethane fraction, and Compound **3** exhibited a 55%, 59%, and 73% chemosuppression (parasite clearance), while the crude extract and dichloromethane fraction showed 39.99% and 52% clearance of parasite respectively in the curative assay. Differential binding preferences were observed for Compounds **1**, **2**, and **3.**Compound **3** was preferentially favoured in displaying strong binding energetics ranging from -7.6 kcal/mol to -10.3 kcal/mol with seven critical protein targets.

Conclusion

This study investigated the antiplasmodial activity of the crude extract and dichloromethane fraction of *A. altilis* stem bark.This is the first report identifying Artocarpentanol (**3**) as a putative antimalarial agent, thereby contributing to the chemistry of the genus

Keywords

Artocarpusaltilis, Artocarpentanol 24(25)-Dihydronorstigmasterol, Stigmasterol, Antiplasmodial activities, molecular and binding energetics.

1. Introduction

Malaria remains one of the most dreaded tropical diseases ravaging the continent of Africa. It is an anopheles' mosquito-borne disease affecting both humans and animals, with clinical manifestations occurring within days of infection. In 2020, about 245 million cases and more than 627, 000 deaths were reported globally; while in 2021, 247 million cases and 625, 000 deaths were reported. It has been estimated that 90% of the cases were from Africa with pregnant mothers and children below the age of 5 the most affected. The emergence of resistant strains of plasmodium coupled with the rapid spread of *Anophelesstephensi* (a vector both of *Plasmodiumfalciparum* and *Plasmodiumvivax* found in India and Sri Lanka) into the African sub-Saharan region introduces a new challenge to the control measures of malaria in Africa [1,2]. This therefore necessitates the investigation of plants for cheap and affordable antimalarial candidates. The use of medicinal plants as antimalarials in healthcare system in Africa and Asia predates the introduction of orthodox drugs. The genus *Artocarpus* J.R. Forst. & G. Forst. consists of deciduous evergreen trees renowned as a source of food, timber and clothing. [3]. *Artocarpusaltilis* (Parkinson ex F.A.Zorn) Fosberg is known as Breadfruit plant in English, it is by the Yoruba ethnic group of South-western Nigeria as a substitute for yam in time of food scarcity, but recently, it has become a staple food [3,4]. Different parts of *A. altilis* are used by the traditional healers among the Yorubasfor the management of various human health conditions including malaria (personal communication) [4,7]. The extracts of various parts of *A. altilis*have been found to exhibit some biological activities, such as protective effect against heart diseases [5-9], neutralisation of harmful radicals in the body, in addition to anti-infective and antimalarial activities against invasive pathogenic microorganisms [8-10]. Recently, the skin protective properties of the plant extract against harmful UVB have been studied [11]. Previous chemical profiling and chromatographic analyses of extracts of *A. altilis* have identified secondary metabolites such as flavonoids of different chemical structures, diels-alder products, terpenoids, arylbenzofuran, neolignans, polyphenolic acids, and prenylflavonoids [12-17].

In furtherance of the investigation of *A.altilis* [17], we reported two phytosteroidal compounds (**1** and **2**) and a flavonoidal compound (**3**) from the hexane-dichloromethane extract of the

hydroalcoholic stem bark extract of *A. altilis*. The antiplasmodial activity of the crude extract, dichloromethane (DCM) fraction and isolated compound, **3**, was also evaluated. In the computational studies, the isolated compounds **1-3** were screened against a total of fifty-four (54) malaria macromolecular targets involved in the pathogenesis of malaria. This was with a view to investigating the ethanolic extract, DCM fraction of the plant for potential antimalarial property.

2. Methods

2.1 General Experimental Procedures

The ^{1}H spectra were recorded on a Varian Inova 600 MHz and 300 MHz while ^{13}C NMR was acquired on 150 and 75 MHz spectrometer. Chemical shifts (δ) were reported in ppm relative to TMS internal standard and coupling constant (*J*) in Hertz with DMSO-d6 and $CDCl_3$ (Sigma-Aldrich Chemie GmbH, Taufkirchen, Germany). The isolated compounds were analysed by the LC-MS Facility of Central Analytical Unit, Stellenbosch University, South Africa. A high-resolution electrospray ionization mass spectrometry (HRESI-MS) fitted with Quadrupole Time-of-Flight (QToF) Synapt G2 Mass Spectrometer (Walters Corporation, Milford, USA) was used to acquire the molecular weights of the compounds in the positive ion mode over a scan range of m/z 100-900. Column chromatographic fractionation was performed using silica gel of mesh sizes 60 (230-400 and 200-400 ASTM, Merck, USA). Column fractions were analysed by TLC on aluminium backed pre-coated silica gel 60 F_{254} 0.2mm. Pure compounds were detected as single spots in UV Chamber dual wavelengths of 254 nm and 366 nm, and by activation with 10% H_2SO_4 and heat. The m.p. of compounds was determined on a Gallenkamp MPD350-BM 3.5 electrothermal instrument (Gallenkamp Kent, UK) working capacity of 220-240V, 50Hz, and 0.3A.

2.2 Plant Collection and Voucher Specimen Deposition

The stem barks of *Artocarpusaltilis* werecollected from the wild (Olosara and Alaro Farm Settlements, 7° 53′41.71N and 4° 58′55.26E) in July 2019. The herbarium specimen was deposited at the Faculty of Pharmacy Herbarium, Obafemi Awolowo University, Nigeria, with voucher number: FPI 2253. The name of the plant was confirmed on the website, www.worldfloraonline.org. [18]. The barks were then dried and milled.

2.3 PreparationofExtractandIsolation

The powdered stem bark (700 g) was macerated with 80% (v/v) aqueous ethanol (7 L) at room temperature for 48 hours with agitation on a Hoover MK IV Motor Shaker. The extract was filtered through cotton plug and clarified by vacuum filtration. It was then concentrated to dryness at 40 °C *in vacuo* on a R110 Rotary Evaporator (Buchi) to yield the crude extract, which was then extracted with 3.5 L of hexane:dichloromethane (30:70) and evaporated to dryness under reduced pressure. The DCM extract was then subjected to open column chromatographic fractionation using silica gel as the stationary phase followed by elution with petroleum spirit with increasing DCM up to 100% followed by gradient with increasing proportion of MeOH up to DCM:MeOH (50:50) to afford nine sub-fractions, DFI-DFIX. Sub-fraction DF I was further fractionated on open column and gradiently eluted with hexane, followed by increasing proportion of DCM up to hexane-dichloromethane (1:1) to afford three sub-fractions DF Ia-c. Sub-fraction DF Ia and DF Ib were combined (similar TLC profile), purified over Sephadex LH-20 column and eluted with DCM-MeOH (8:2) to afford Compound **1** as a white powder (20 mg). Sub-fraction DF II was similarly chromatographed on open column using silica gel 60-120 mesh size as stationary phase to afford Compound **2** as an off-white solid (23 mg), sub-fractions DF IV-DF IX were pooled together (similar TLC profile), fractionated over sephadex LH 20 column and eluted isocratically with DCM:MeOH (7:3) to give a dark-yellow powder (47 mg) on evaporation of the solvent, which was then purified by recrystallization from chloroform to give a bright yellow powder and termed Compound **3**.

2.4 Antiplasmodial Activity of Extract, DCM fraction and Compound 3

2.4.1 Acute Oral Toxicity of Crude Extract

This was carried out in accordance with the Organisation for Economic Cooperation and Development OECD 425 guidelines [19]. Overnight-fasted non-infected mice (n=7) were dosed with 2000 mg/kg of the crude extract by oral gavage. The animals were then allowed free access to water only, while the feed was withdrawn for 3 hours. The animals were then observed for 1hour post administration of extract for immediate toxicity signs and then for 24 hours (every 4 hours intermittently). The animals were then monitored for 14 days for toxic behavioural reactions.

2.4.2 Animal Handling and Parasite Strain

Plasmodiumberghei NK 65 (chloroquine-sensitive) strain used in this research was obtained from Institute for Malaria Research and Training (IMRAT), University College Hospital Ibadan, Nigeria. The parasite was maintained by serial passaging of blood from infected mice (donor mice) to non-infected mice. All animal experimental procedures were carried out as approved by the Postgraduate Board of research Obafemi Awolowo University with number PHP17/18/H/0970. Mice of either sexes with weight ranging from 18 to 22 g obtained from Animal House of the Department of Pharmacology, Obafemi Awolowo University were allowed to acclimatised in the laboratory for 2 to 3 days before use and allowed access to standard animal chow (Breedwell) and water ad libitum.

2.4.3 Inoculum Preparation

Parasitized blood sample was harvested from the donor mice through cardiac puncture was diluted in *n*-saline using standard protocol such that 0.2 mL of inoculum corresponds to 1×10^7 parasitized erythrocytes. Dilution was done according to the number of mice to be innoculated.

2.4.4 Animal Study Design

Three different antimalarial assays were carried out, namely; suppressive, prophylactic and curative assays. The experimental procedures are described below:

2.4.5 The 4-day Suppressive Assay

Evaluation of the schizonticidal activity of the crude extract, DCM fraction and compound **3** on early infection was carried out in accordance with the method of Imran *et al*. [20]. Animals were divided into nine groups of five mice each (n = 5). Group I was tagged negative control (NC) – receiving 0.2 mL *n*-saline. Groups II, III and IV were tagged crude extract (CE) groups – receiving 100 mg/Kg, 200 mg/Kg and 400 mg/Kg of crude extract respectively, while, Groups V, VI and VII were tagged DCM fraction groups – receiving 100 mg/Kg, 200 mg/Kg and 400 mg/Kg of DCM fraction respectively. Group VIII was tagged Compound **3** – receiving 10 mg/Kg of Compound **3** while group IX was tagged positive control – receiving 10 mg/Kg chloroquine (CQ). After a standard protocol of parasite inoculum preparation, the animals were intraperitoneally inoculated with 0.2 mL inoculum size containing 1.0 X 10^7 parasitized

erythrocytes. Treatment started after 2 hours and was done once daily for 4 days: day 0, 1, 2 and 3 post-inoculations. All drug administration was done orally. Blood was collected from the tail of each mouse on day 4 post-inoculation and a thin smear was prepared using standard protocols. The percentage parasitemia and chemosuppresive effect were determined using the equation:

$$\%parasitemia = \frac{numberofparasitisedRBCs}{totalnumberofRBCs} \times 100$$

While the % suppression = $\frac{A-B}{A}$ where A is the mean parasitemia of negative control and B is the mean parasitemia of treated groups and positive control. The animals were observed daily for their survival time.

2.4.6 Prophylactic Assay

The residual infection protocols as described by Peters [21] was used. The prophylactic activity of crude extract and DCM fraction were evaluated. Mice were divided as stated above excluding Compound **3** due to low yield. The positive control group-chloroquine (CQ) took the position of group VIII. Accordingly, appropriate doses of the drug agents were orally administered to the corresponding groups for 3 days: day 0, 1 and 2. On day 3, all mice were then innoculated with 0.2 mL of inoculum which corresponds to 1×10^7 parasitized erythrocytes. After 72 hours post-infection, a thin blood smear of each mouse was prepared using standard protocols and parasitemia level was determined. The animals were observed for 28 days for their survival time.

2.4.7 Rane's Curative Test

The curative effect of crude extract and DCM fraction on an established infection was evaluated following the method of Ryley and Peters [22]. Animals were randomly grouped as described in prophylactic assay and were infected with 0.2 mL standardised inoculum of 1×10^7 parasitized erythrocytes and the infection was allowed to develop for 72 hours while the animals were allowed free access to feed and water. Treatment started 72 hours post-infection and continued daily for 5 days using the doses earlier stated. The parasitemia level was assessed daily throughout the treatment period and the survival time was determined.

2.4.8 Statistical Analysis

Data were expressed as mean and standard error of the mean using Microsoft excel software and analysed on GraphPad Prism 5.0 using one-way ANOVA followed by Tukey post hoc for the comparison of the mean % parasitemia and survival time. Results of $P<0.05$ were considered significant.

2.5 Computational modelling investigation

In order to obtain an atomistic level insight into the interaction between each of the three constituents and disease-relevant macromolecular targets in clinically significant *Plasmodium falciparum* infection, 3D models of Compounds **1**, **2** and **3** in SDF format were retrieved from www.pubchem.org, a global repository of curated organic compounds. The models were converted to PDBQT formats with partial atomic charges computed and incorporated. We assembled a total of fifty-four (54) macromolecular targets (**Table 1**) that have been implicated in malaria infection. The elected protein targets included twenty unique crystallographic models with some of them involving multiple models (e.g. plasmepsin II) as well as multiple binding subsites (e.g. duptase) especially where different co-factors have been implicated for enzyme activity

Table 1: Macromolecular models employed for docking screening.

Macromolecular target index	**Name**	**Detail of docking model**
Target 1, 2	Aspartate transcarbamoylase	2 models
Target 3	Di-adenosinetriphydrolase	1 model
Target 4, 5	Dihydrofolate reductase thymidylate synthase	2 models
Target 6-9	Dihydroorotate dehydrogenase	4 models
Target 10	Duptase	1 model, 3 sites

Target 11, 12	Duptase	2 models
Target 13,14	Eoyl-ACP-reductase	2 models
Target 15,16	Fkbp35	1 model 2 sites
Target 17	Fructose *bis*phosphate aldolase	1 model
Target 18,19	Glutathione-S-transferase	1 model 2 sites
Target 20	Lactate dehydrogenase	1 model
Target 21	NADH-ubiquinone oxidoreductase	1 model 3 sites
Target 24	Nicotinic acid monocleotide adenylyltransferase	1 model
Target 25,26	Orotidine-5-monophosphate decarboxylase	1 model 2 sites
Target 27-29	Pfck2	1 model 3 sites
Target 30,31	Pfpka-R141-441	1 model 2 sites
Target 32-34	Prolyl-*t*RNA synthetase	2 models, 2sites
Target 35	Purine nucleoside phosphorylase V181D mutant	1model
Target 36-44	Triose phosphate isomerase	4 models, 3 sites
Target 45-50	Plasmepsin II	6 models

After downloading the 3D crystallographic files (www.rcsb.org) extraneous molecules (e.g. employed for the crystallographic process but not directly involved in inhibitor or substrate interaction) were removed after which coordinates of appropriate co-crystallized substrates and

inhibitors were seperated to serve as reference standard for in the subsequent docking screen. Hydrogen atoms and Gasteiger charges were added using Autodock Tool [23] after which docking grids were automatically constructed for each target using in-house programme developed for this purpose. The automatic computation of docking grid utilizes the coordinates of co-crystallized ligand in computing a 3D docking grid centered at the geometric center of mass of the ligand with edges padded in all directions with varying values but typically 1.5 A. The docking screen employed Autodock Vina [24,25] at an exhaustiveness value of 8 and with each of Compounds **1**, **2** and **3** docked into the identified binding sites of the fifty-four macromolecular models. The top predictions in all 216 docking iterations (including 162 for the target compounds) were collected and analyzed.

3. Results

3.1 Spectroscopy data of Compounds

Compound 1 (Stigmasterol, $C_{29}H_{48}O$)

Nature: colourless or white powder

Melting point: 162-164°C

Yield: 20 mg with R_f of 0.29 in hexane-dichloromethane (3:7)

^{1}H-NMR (600 MHz, $CDCl_3$) and ^{13}C-NMR (150 MHz, $CDCl_3$): Table 2

Table 2: Spectroscopic Data of Compound 1 compared with Stigmasterol

Position	Compound 1		Stigmasterol [26, 27]	
	δ_H (ppm)	δ_C (ppm)	δ_H (ppm)	δ_C (ppm)
1		37.41		37.6
2		31.85		32.1
3	3.52, 1H, m, 6.6 Hz	72.19	3.51, 1H, tdd	72.1
4	2.31;1.86, 2H, d, 6.5 Hz	42.46		42.4
5		140.93		141.1
6	5.35,1H, bs, 1.6 Hz	122.09	5.31, 1H, t	121.8
7		31.85		31.8
8		32.06		31.8
9		50.30		50.2
10		36.06		36.6
11		21.24		21.5

12		39.84		39.9
13		42.48		42.4
14		56.43		56.8
15		24.47		24.4
16		28.40		29.3
17		56.22		56.2
18	1.01, 3H, s	12.01	1.03, 3H, s	12.2
19	0.68, 3H, s	19.13	0.71, 3H, s	18.9
20		40.63		40.6
21		19.19	0.91, 3H, d, 6.2 Hz	21.7
22	5.17, 1H, m, 8.7 Hz	138.67	5.14, 1H, m	138.7
23	5.03, 1H, m, 8.6 Hz	129.65	4.98, 1H, m	129.6
24	0.84, 1H, m, 6.7 Hz	51.60		46.1
25		36.30		25.4
26		12.13	0.83, 3H, t	12.1
27	0.82, 1H, m, 6.8 Hz	25.55		29.6
28	0.92, 3H, d, 6.5 Hz	19.55	0.82, 3H, d, 6.6 Hz	20.2
29	0.91, 3H, d, 6.5 Hz	18.93	0.80, 3H, d, 6.6 Hz	19.8

Chemical shifts of proton and carbon signals are presented in parts per million (ppm) in deuterated chloroform, s, d, dd, m, bs, tdd, t, respectively stands for singlet, doublet, doublet of doublet, multiplet, broad singlet, triplet of doublet of doublet, and triplet respectively

Compound 2 (24(25)-dihydronorstigmasterol, $C_{28}H_{46}O$)

Nature: colourless white powder

Melting Point: 140-141°C

Yield: 23 mg with R_f of 0.33 in hexane-dichloromethane (3:7)

^{1}H-NMR (300 MHz, $CDCl_3$) and ^{13}C-NMR (75 MHz, $CDCl_3$): Table 3

HRESI$^+$TOF-MS: m/z 421.1286 ($M+Na^+$) calculated for $(C_{28}H_{46}O)^+$, 398.6142

Table 3: Spectroscopic Data of Compound 2 (24(25)-dihydronorstigmasterol)

Position	**Compound 2**		**DEPT Analysis**
	δ_H (ppm)	**δ_C (ppm)**	**Multiplicity**
1		29.07	CH_2
2		31.82	CH_2
3	3.56, 1H, m,	71.92	CH
4	2.33; 1.95, 2H, d, 6.0 Hz	42.46	CH_2
5		140.91	C
6	5.35, 1H, bs, 5.2 Hz	121.88	CH
7		28.40	CH_2

8		32.06	CH
9		50.31	CH
10		37.41	C
11		21.37	CH_2
12		36.66	CH_2
13		45.99	C
14		56.92	CH
15		26.22	CH_2
16		25.56	CH_2
17		57.02	CH
18	0.85, 3H, s	23.22	CH_3
19	0.82, 3H, s	21.24	CH_3
20		36.30	CH
21	0.71, 3H, d, 6.7 Hz	19.55	CH_3
22	1.31, 2H, m, 6.0 Hz	32.06	CH_2
23	1.43, 2H, m, 6.2 Hz	29.30	CH_2
24		138.47	C
25		129.43	C
26	1.01, 3H, s	19.13	CH_3
27	1.01, 3H, s	19.18	CH_3
28	0.93, 3H, d, 6.1 Hz	12.41	CH_3

Chemical shifts of proton and carbon signals are presented in parts per million (ppm) in deuterated chloroform, s, d, dd, m, bs, tdd, t, C, CH, CH_2, CH_3, respectively stands for singlet, doublet, doublet of doublet, multiplet, broad singlet, triplet of doublet of doublet, triplet, quartenary, methine, methylene, and methyl carbon atoms.

Compound 3 (Artocarpentanol, $C_{15}H_{10}O_7$)

Nature: yellow powder

Melting Point: 316-318°C

^{1}H-NMR (300 MHz, DMSO-d_6) and ^{13}C-NMR (75 MHz, DMSO-d_6): Table 4

Table 4: Spectroscopic Data of Compound 3 compared with Artocarpentanol A

Position	Compound 3		Artocarpentanol A [17]	
	δ_H (ppm)	**δ_C (ppm)**	**δ_H (ppm)**	**δ_C (ppm)**
2		136.50 C		136.47
3		157.05 C		157.02
4		176.48 C		176.45
4a		109.57 C		109.55
5		157.13 C		157.10
6	6.30, 1H, d	93.70 CH	6.29, 1H, s	93.68
7		163.96 C		163.94

8	6.18, 1H, d	98.39 CH	6.17, 1H, s	98.36
8a		149.27 C		149.26
1’		103.84 C		103.82
2’		160.71 C		160.69
3’	6.39, 1H, dd, 8.5Hz	103.27 CH	6.39, 1H, d, 7.4 Hz	103.25
4’		161.20 C		161.18
5’	6.35, 1H, 2Hz	107.20 CH	6.35, 1H, dd, 7.1 Hz	107.10
6’	7.22, 1H, d, 8.3Hz	132.03 CH	7.23, 1H, d, 7.3 Hz	131.99
-	12.58, 1H, s	-	12.59, 1H, s	-

Chemical shifts of proton and carbon signals are represented in parts per million (ppm) in deuterated chloroform, s, d, dd, m, bs, tdd, t, respectively stands for singlet, doublet, doublet of doublet, multiplet, broad singlet, triplet of doublet of doublet, and triplet

3.2 Antiplasmodial Activities of Extract, Fraction and Compound

The antiplasmodial activities of the crude extract, DCM fraction, isolated compounds, standard antimalarial drug (chloroquine) as the positive control and infected but untreated mice as negative controls are presented in Tables 5-7 respectively.

Table 5: Antiplasmodial Activity of Crude Extract, Fraction and Compound 3 in 4-day Suppressive Test

Test Groups	% Parasitemia ± SEM	% Suppression	Survival Time ± SEM
NC	$57.83\pm0.35^{apq*}$	0.00	$6.25\pm0.39^{apq*}$
CE (100 mg/kg)	$42.79\pm0.55^{apbq*}$	26.00	$8.55\pm0.51^{abpq*}$
CE (200 mg/kg)	$34.31\pm1.25^{abq*}$	40.67	$11.89\pm0.95^{abq*}$
CE (400 mg/kg)	$25.91\pm0.62^{abp*}$	$55.19^{a}*$	$13.51\pm0.37^{ab*p}$
DCM (100 mg/kg)	$37.75\pm0.47^{apbq*}$	34.72	$9.65\pm0.18^{abqp*}$
DCM (200 mg/kg)	$29.95\pm0.37^{abq*}$	48.21	$12.91\pm0.77^{abq*}$
DCM (400 mg/kg)	$23.55\pm0.83^{ab*p}$	$59.28^{a}*$	$14.63\pm0.39^{abp*}$
3 (10 mg/kg)	$15.37\pm1.78^{abpq*}$	73.42	$19.45\pm0.81^{abpr*}$
CQ (10 mg/kg)	0.95 ± 0.15^{pqb}	98.36	$28.00\pm0.00^{bpq*}$

Data are expressed as mean ± SEM (standard error of mean), n=5. NC, negative control received 0.2 ml n-saline; CE and DCM, crude extract and dichloromethane fraction of *A. altilis* stem bark at 100, 200, 400 mg/kg dose levels: $^{*}p<0.05$, Compound 3 and CQ (chloroquine) were tested at dose of 10 mg/kg. a, compared to CQ; b, compared to NC; p, q compared to 200, 400 mg/kg doses respectively.

Table 6: Antiplasmodial Activity of Crude Extract and Fraction of *A. altilis* Stem Bark in Rane’s Test

Test Groups/Doses	% Parasitemia ± SEM	% Suppression	Survival Time ± SEM
NC	$57.83\pm0.35^{apq*}$	0.00	$6.25\pm0.39^{aqp*}$
CE (100 mg/kg)	$53.39\pm0.25^{abpq*}$	7.70	$7.09\pm0.71^{abpq*}$

CE (200 mg/kg)	43.81±0.61^{abq*}	24.27	9.25±0.38^{abq*}
CE (400 mg/kg)	34.71±0.23^{ab*}	39.99	12.62±0.77^{abp*}
DCM (100 mg/kg)	41.55±0.70^{abpq*}	28.15	10.81±0.29^{abqp*}
DCM (200 mg/kg)	38.35±0.49^{abq*}	33.69	12.91±0.97^{abq*}
DCM (400 mg/kg)	27.65±0.81^{bap*}	52.19 ^{a}*	14.91±0.45^{abq*}
CQ (10 mg/kg)	3.07±0.53^{bpq*}	94.71	28.00±0.00^{bpq*}

Data are expressed as mean ± SEM (standard error of mean), n=5. NC, negative control received 0.2 mL *n*-saline; CE and DCM, crude extract and dichloromethane fraction of *A. altilis* stem bark at 100, 200, 400 mg/kg dose levels: $^{*}p<0.05$, Compound 3 and CQ (chloroquine) were tested at dose of 10 mg/kg. Compound **3** was not tested for the curative antimalarial assay due to the low yield of the compound. a, compared to CQ; b, compared to NC; p, q compared to 200, 400 mg/kg doses respectively.

Table 7: Antiplasmodial Activity of Crude Extract and Fraction of *A. altilis* Stem Bark in Prophylactic Test

Test Groups/Doses	% Parasitemia ± SEM	% Suppression	Survival Time ± SEM
NC	57.83±0.35^{aqp*}	0.00	6.25±0.39^{apq*}
CE (100 mg/kg)	55.74±1.53^{bp**aq*}	3.71	7.09±0.71^{abpq**}
CE (200 mg/kg)	52.22±0.19^{abq*}	9.72	8.39±0.58^{abq*}
CE (400 mg/kg)	50.11±0.70^{abp**}	13.35	10.71±0.57^{abp*}
DCM (100 mg/kg)	55.92±0.90^{abpq**}	3.30	7.31±0.90^{abpq**}
DCM (200 mg/kg)	53.19±0.20^{abq**}	8.02	7.91±0.59^{abq**}
DCM (400 mg/kg)	49.95±0.75^{abp*}	13.63	11.15±0.50^{abp*}
CQ (10 mg/kg)	9.07±0.53^{bpq*}	85.31	28.00±0.00^{bpq*}

Data are expressed as mean ± SEM (standard error of mean), n=5. NC, negative control received 0.2 mL *n*-saline; CE and DCM, crude extract and dichloromethane fraction of *A. altilis* stem bark at 100, 200, 400 mg/kg dose levels: $^{*}p<0.05$, $^{**}p<0.001$. Compound 3 and CQ (chloroquine) were tested at dose of 10 mg/kg. Compound **3** was not tested for the prophylactic antimalarial assay due to the low yield of the compound. a, compared to CQ; b, compared to NC; p, q compared to 200, 400 mg/kg doses respectively.

3.3 Docking analysis: Interaction of Compounds with Molecular targets

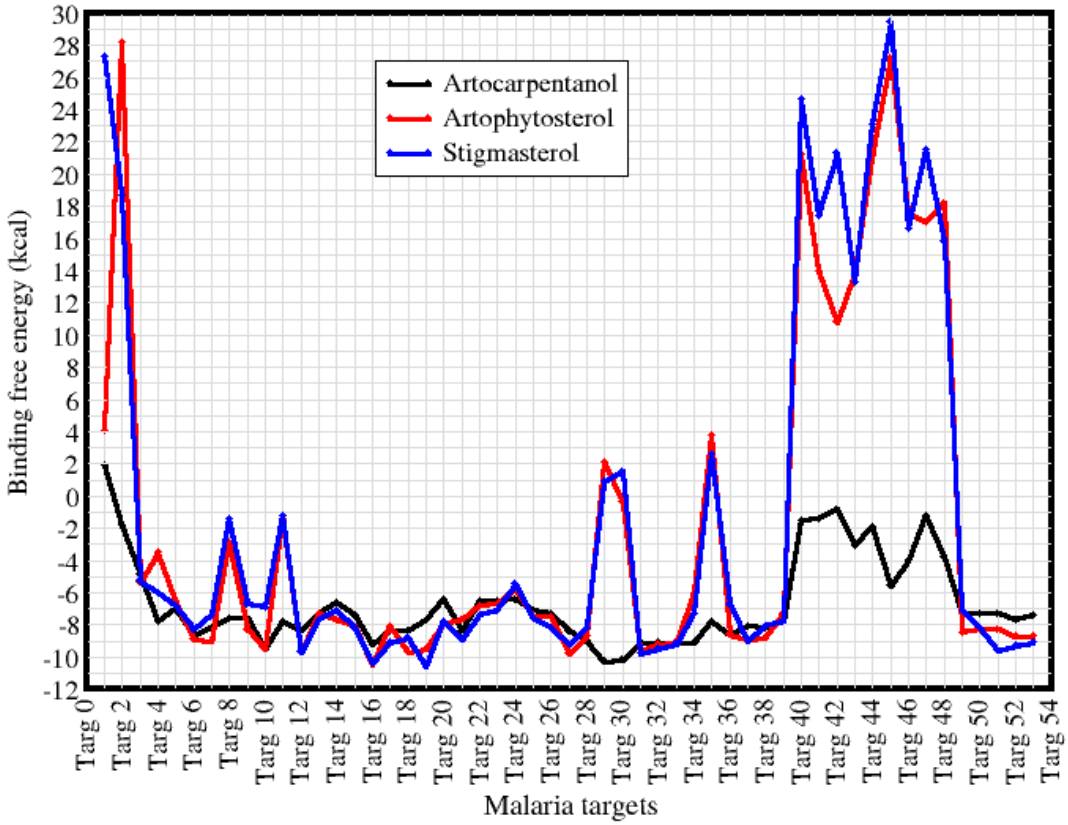

Figure 1: Docking scores for Compounds 1, 2, and 3 against 54 malaria macromolecular targets.

4. Discussion

4.1 Spectra interpretation

Compound **1** was isolated from the dichloromethane fraction as a white powder with a melting point of 162-164 °C. It appeared as a pink colouration when the TLC chromatogram was sprayed with 10% H_2SO_4 and on heating at 100 °C. Fromthe proton spectrum of **1**, three proton peaks in the olefinic region at δ values 5.35 ppm (1H, bs, H-6); 5.17 ppm (1H, m, H-22); 5.03 ppm (1H, m, H-23). The signal at 3.52 ppm (1H, m, H-3) is a sp^3 methine (CH) attached to an electronegative oxygen, by bonding electron withdrawal, causing the proton signal to resonate downfield from the aliphatic region. Furthermore, many signals with much overlapping in the

aliphatic region 0.50-2.50 ppm, indicating the steroidal hump of Compound **1**, consisting of 2.31 ppm (1H, d, 6.4 Hz, H-4); 1.86 ppm (1H, d, 6.5 Hz, H-4); characteristic singlets of angular methyl groups 1.01 ppm (3H, s, H-18) and 0.68 ppm (3H, s, H-19); and a typical isopropyl moiety consisting of 0.92 ppm (6H, d, 6.5 Hz, H-28 and H-29) and 0.82 ppm (1H, m, 6.8 Hz, H-27); 0.84 ppm (1H, d, 6.7 Hz, H-24).From carbon spectrum of Compound **1,** four non-equivalent carbon signals were observed in the olefinic region, indicating that **1** has four sp^2-hybridized olefinic carbon atoms with δ values 140.93 ppm (C-5); 138.67 ppm (C-23); 129.65 ppm (C-22) and 122.09 ppm (C-6), sp^3 hybridized oxygenated methine signal at δ 72.19ppm (C-3) and many signals in the region 10-60 ppm typical of a steroidal compound. The Attached Proton Test spectrum of **1** showed three quartenary carbons atoms, comprising one olefinic carbon δ 140.93 ppm, therefore confirming that carbon signals 138.67 ppm (C-23); 129.65 ppm (C-22) and 122.09 ppm (C-6) respectively are protonated olefinic methine carbons. The spectrum also showed signals eight sp^3-hybridized carbon atoms, nine sp^3-hybridized methylene (CH_2) and six methyl (CH_3) groups. The COSY, HSQC and HMBC spectra of **1** showed a correlation between 72.19 ppm and 3.52 ppm, which shows the hydroxylated methine carbon C-3 of **1**. The available spectroscopic data on Compound **1** agrees with the literature data on Stigmasterol according to Shah and Khan [26] Based on this evidence, Compound **1**was termed Stigmasterol, which is reported for the first time from *Artocarpusaltilis* stem bark extract.

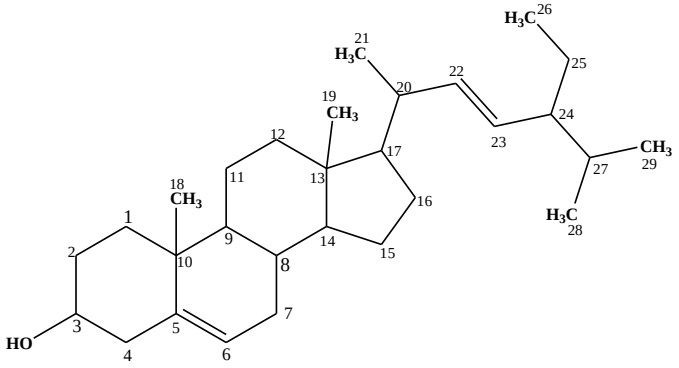

Figure 2: Structure of Compound 1

Compound **2**, 24(25)-dihydronorstigmasterol was also isolated from the dichloromethane fraction as a white powder with a melting point of 140-141°C, showing Compound **2** is different from **1**. It appeared as a purplish-pink colouration when the TLC chromatogram was sprayed with 10% H_2SO_4 and heated to 100 °C. In^{1}H-NMR spectrum of **2**, only one signal in the olefinic

region at δ values 5.36 ppm (1H, bs, H-6) was observed unlike Compound **1**. A signal at 3.56 ppm (1H, m, 6.5 Hz, H-3) is an sp^3-methine proton attached to an electronegative oxygen, causing the deshielding effects by bonding electron withdrawal. The spectrum also showed many signals with much overlapping in the aliphatic region from 0.5-2.5 ppm, indicating the steroidal nucleus of **2**, consisting of 2.33 ppm (1H, d, 5.9 Hz, H-4); 1.95 ppm (1H, d, 6.0 Hz, H-4); characteristic singlets angular methyl groups 0.85 ppm (3H, s, H-18) and 0.82 ppm (3H, s, H-19); and a dimethyl moiety consisting of 1.01 ppm (6H, s, H-26 and H-27), 0.93 ppm (3H, d, 6.1 Hz, H-28); 1.31 ppm (2H, m, 6.0 Hz, H-22), 1.43 ppm (2H, m, 6.2 Hz, H-23), 0.71 ppm (3H, d, 6.7 Hz, H-21) among other signals. The ^{13}C-NMR spectrum of **2** showed four non-equivalent carbon signals in the olefinic region indicating that Compound **2** has four sp^2-hybridized olefinic carbon atoms with δ values 140.91 (C-5); 138.47 (C-24); 129.43 (C-25) and 121.88 (C-6), comparing the carbon spectrum with DEPT spectrum of **2,** showed that three olefinic carbon signals 140.91 (C-5); 138.47 (C-24); 129.43 (C-25) are quartenary carbons (having no protons attached). This distinguishes Compound **2** from **1**. The spectrum further showed sp^3-hybridized oxygenated methine signal at δ value 71.96 ppm (C-3) and many signals in the region 10-60 ppm typical of steroidal compound. The combination of ^{13}C and DEPT spectra of **2** showed that **2** contains seven methine carbon atoms comprising one methine olefinic carbon atom C-6 at δ value 121.88 ppm and six other sp^3-hybridized methine carbon atoms, which particularly distinguishes **2** from **1**. Furthermore, eleven sp^3-hybridized methylene carbon atoms and six methyl groups resonated as five sp^3 hybridized methyl carbon signals. The COSY, HSQC and HMBC spectra of **2** confirmed correlations between 71.96 ppm and 3.56 ppm, which shows the hydroxylated methine carbon C-3 of Compound **2**. The carbon signal due to C-6 at δ value 121.88 ppm correlates with the proton signal at δ value 5.36 ppm, indicating the only olefinic methine protonated carbon in the molecule. The information obtained on Compound **2** differs from Sitosterol in possessing the second olefinic double bond of C-24 and C-25. Hidayathulla et al. [27] reported the isolation of Sitosterol from *Schimperaarabica*. Therefore, **2**has been named 24(25)-dihydronorstigmasterol, which to the best of our knowledge, is reported for the first time from *Artocarpusaltilis* stem bark. The MS spectrum of **2** showed m/z 421.1286 as the chemically ionized (sodiated) molecular ion peak $M+Na^+$ of 37% abundance, which corresponds to the molecular ion M^+ 398.6142, and m/z 274.2749 as the base peak having the highest % abundance in the spectrum. The peak is a result of the bond scission of the cyclohexene ring of the steroidal

skeleton involving C-6(7)-C-9(10) to generate a radical cation $[C_{20}H_{34}]^+$. The spectrum also showed other fragment ions, which include m/z 230.2488 (83%), 217.0695 (23%), 186.2225 (46%), 179.0186 (33%), 157.0364 (31%).

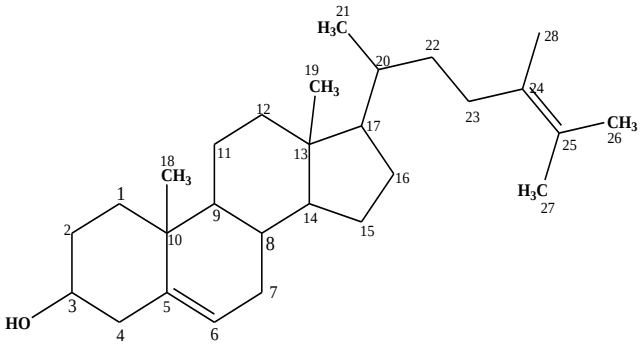

Figure 3: Structure of Compound 2

Compound **3** was recrystallized from chloroform as a yellowish powder. Spectroscopic structure elucidation and comparison with literature confirmed **3** to be Artocarpentanol A, which was reported from *A. altilis* [17]. In the ^{1}H-NMR spectrum of **3**,no sp^3-hybridized aliphatic protons were seen in the spectrum of **3**. The signal δ 12.58 ppm (1H, s) which is due to flavonoidal skeleton of **3**. Five benzenoid protons were observed with δ values 7.24 ppm (1H, d, 8.3 Hz, H-6'), 6.39 ppm (1H, dd, 8.5 Hz, H-3'), 6.35 ppm (1H, dd, 2 Hz, H-5'), 6.30 ppm (1H, d, H-6) and 6.18 ppm (1H, d, H-8). Inspection of ^{13}C spectrum showed peaks for fifteen chemically different carbon atoms. The spectrum showed quartenary carbonyl carbon at δ value 176.48 ppm, while oxygenated or hydroxylated sp^2-hybridized carbon atoms at δ values 163.96 ppm to 149.27 ppm. The COSY spectrum of **3** showed the $^3J_{H-H}$ homonuclear coupling between 7.24 ppm and 6.39 ppm while the $^1J_{C-H}$ and $^3J_{C-H}$ heteronuclear couplings of **3** are shown by HSQC and HMBC spectra. The mass spectrum and elemental composition data of **3** revealed the molecular formula to be $C_{15}H_{10}O_7$ with 11 unsaturation index. The ion m/z 303.0512 is the base peak with highest % abundance and molecular ion ($M+H^+$) along with m/z 304.0545, 305.0561 and 325.0332 due to $M+2H^+$, $M+3H^+$ $M+Na^+$ respectively.

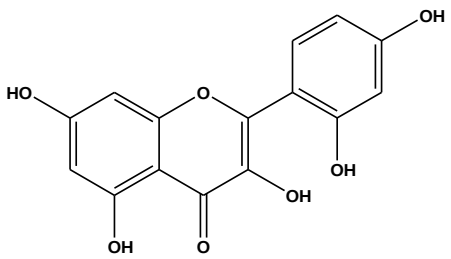

Figure 4: Structure of Compound 3

4.2 Toxicity and Antiplasmodial Activities

Results obtained on the acute oral toxicity showed that no mortality was observed in treated animals throughout the period of observation. No unusual or abnormal behavioural changes were observed in the treated animals. The antimalarial activities of all treated groups increases with increasing dose levels (dose-dependent). The highest % reduction of parasitaemia load of infected mice (% suppression) was observed at 400 mg/kg for the extract and DCM fraction for the 4-day suppressive, established infection and residual tests respectively. Compound **3** exhibited a significant ($P<0.05$) antimalarial activity than the crude extract and DCM fraction with a 73% suppression at 10 mg/kg compared with standard drug, chloroquine tested at the same dose with a 98% suppression of the parasite load. The result further showed that fractionation and partitioning enhanced the antiplasmodial activity as evident from the clearance of the parasite from blood of infected mice followed the order: chloroquine > Compound **3**> DCM fraction > crude extract. There is a significant difference ($P<0.05$)in the % parasitemia and survival time between the treated groups and control groups for the 4-day suppressive, curative and prophylactic tests respectively. However, no significant difference at $P<0.05$ in the survival time between crude extract (CE) and dichloromethane fraction (DCM) at 200 mg/kg in the 4-day suppressive test. Similarly, no significant difference at $P<0.05$ in the % parasitemia and survival time between CE and DCM fraction in the prophylactic test at 400 mg/kg. Also, the results showed that the crude extract (at 200 and 400 mg/kg), DCM fraction (at 200 and 400 mg/kg), and Compound **3** prolonged the survival days of infected mice, with a corresponding reduction in the parasitaemia as compared to the negative controls. It has been suggested that putative antimalarial compounds must cause a reduction in the parasitaemia by at least 30% [28], thereby making compound **3** a potential antimalarial drug candidate. However, the crude extract, DCM fraction, and compound **3** showed antimalarial activity after administration of the second dose, as

against the standard drug (chloroquine)that showed marked suppression of the parasite after administration of the first dose. This present study agreed with previous reports on the antiplasmodial activities of *A. altilis* [29-31] and proposes Artocarpentanol as a potential antimalarial compound for further investigation.

4.3 Macromolecular receptor interaction from docking screening

Figure **1** presents the free energy of binding values computed for the three compounds across the fifty-four malaria macromolecular targets. In modelling, the possible molecular mechanism(s) underlying the experimentally observed antimalarial activity of compound **3** it was assumed that in vivo there existed little or no barrier to the interaction of molecules of compound **3** with all available plasmodium targets: that is, with the exception of physicochemical and pharmacokinetic barriers. This informed the inclusion of as many macromolecular targets as were considered relevant in determining antimalarial potency. Secondly, the modelling was extended to compounds **1** and **2** to properly contextualize the interaction pattern computed for compound **3**. In Figure 1, the computed affinities of the three compounds were plotted to provide a global glimpse of how the interaction behaviour varied with respect to the isolated compounds and also with respect to the protein targets. While all three compounds showed a viable binding energetics with many of the targets, compound **3** was preferentially favoured in displaying strong binding energetics (approx. -9.0 kcal/mol) with seven critical protein targets. These are targets referenced in Figure 1 as Targ 04, 08, 11, 29, 30, 34 and 35 corresponding to *Plasmodium* dihydrofolate reductase thymydylate synthase, dihydroorotate dehydrogenase, duptase, Pfck2, Pfpka-R141-441, prolyl *t*-RNA synthase, and purine nucleoside phosphorylase V181D. Out of the three isolated compounds, it was only compound **3** that interacted strongly with these seven critical plasmodial macromolecules. With the strong interaction ranging from -7.6 kcal/mol for dihydroorotate dehydrogenase to -10.3 kcal/mol for reductase thymydylate synthase, compound **3** appeared well suited structurally and electrostatically for the seven protein targets. These interactions are additionally important since they represent points of divergence with compounds **1** and **2** and may well explain the superior antimalarial efficacies recorded for compound **3**.

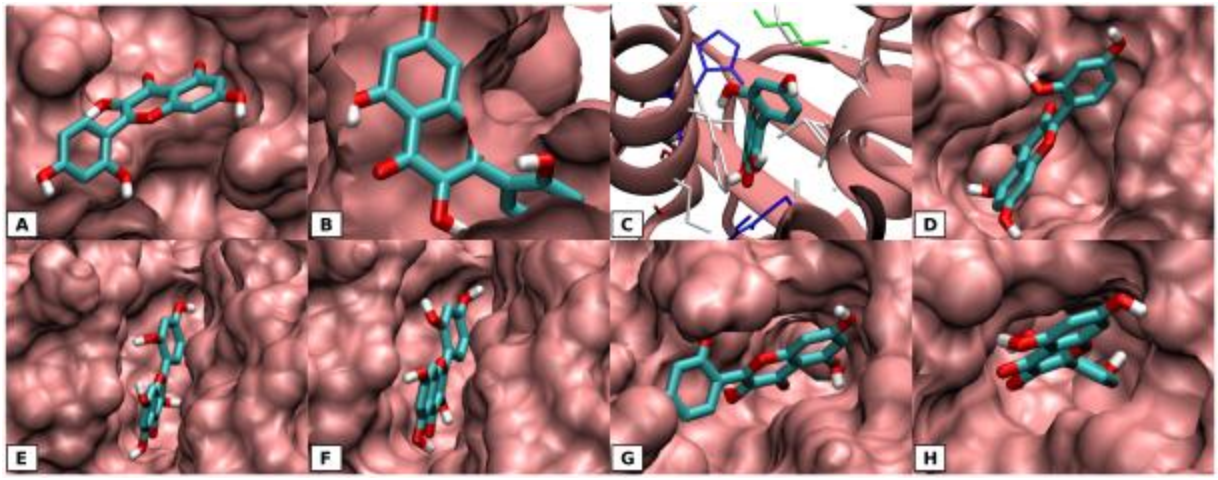

Figure 5: Binding pattern observed for Compound **3** in the binding site of *Plasmodium* dihydrofolate reductase thymydylate synthase (A), dihydroorotate dehydrogenase (B), surface representation), dihydroorotate dehydrogenase (C, cartoon representation), duptase (D), Pfck2 (E), Pfpka-R141-441 (F), prolyl *t*-RNA synthase (G), and purine nucleoside phosphorylase V181D (H).

In order to better characterize the binding interactions exhibited in the seven systems, 3D graphical rendering of the interaction of compound **3** with each of the macromolecular targets was performed (Figure 2). With the exception of dihydrofolate reductase thymydylate synthase (Figure **5[A]**), compound **3** could be seen forming interaction with buried surfaces in water-excluded regions of each molecular target. In the case of dihydrofolate reductase thymydylate synthase, compound **3** could be found interacting at a relatively flat binding surface with a significant portion of compound **3**'s surface area water exposed. One would expect such binding to be only short-lived and be unable to survive structural disturbances under *in vivo* situation. Binding to the other targets on the other hand involve extensive burial inside largely hydrophobic cavities. In the case of dihydroorotate dehydrogenase, compound 3 was bound within a cavity that is completely solve-excluded: the surface of the binding cavity was sliced off in Figure **5[B]** to show the bound ligand. In Figure **5[C]**), the binding cavity was re-represented using cartoon and wire representation. Compound 3 inserted into a predominantly hydrophobic binding cavity composed of two helical units and side-chain amino acids from the helices constitute the binding site. Binding to duptase (Figure **5[D]**), Pfck2 (Figure **5[E]**), Pfpka-R141-441 (Figure **5[F]**),

prolyl *t*-RNA synthase (Figure **5[G]**), and purine nucleoside phosphorylase V181D Figure **5[H]**) involved significant burial within the active site with only a relatively small portion of the bound ligand being exposed to the surrounding water.

Conclusion

This present study reported the structure elucidation of two phytosteroidal compounds and a flavonoid from the dichloromethane extract of *A. altilis* stem bark and evaluated antimalarial activities of the crude extract, DCM fraction and Compound, **3**. In conclusion, the strong interaction of the **3** with seven molecular targets of importance to the pathogenesis of malaria, in addition to the good chemosuppresive activity makes **3**, a potential antimalarial agent.

Abbreviations

DCM, dichloromethane; TLC, thin layer chromatography; TMPs, traditional medical practitioners; r.t., room temperature; Rf, retardation factor; ppm, parts per million.

Funding

This research did not receive any funding or grant from funding agencies in public, private, commercial or not-for-profit sectors.

Declaration and Statements

The authors certify that there is no competing interest to express regarding the content of this article.

Author's Contribution

Conceptualization, Supervision and Administration of Research (JM Agbedahunsi & FO Olorunmola), Data curation, Study design, Methodology, Investigation of Experimental work, Interpretation and Analysis of Results(SB Ogundele & ID Asiyanbola), Resources, NMR and MS Instrumentation (AO Oyedeji & AO Oriola), Computational Studies, Analysis and Writing original draft (OO Olubiyi, K Babalola, BA Yusuf, and EA Agbebi).

All authors approved the final manuscript draft.

Acknowledgements

The authors are grateful to the NMR and MS Units of the Central Analytical Facilities of Stellenbosch University, South Africa, for recording the NMR and HRESIMS spectra of isolated compounds. The authors are also grateful to Afe Babalola University, Ado-Ekiti, Nigeria for sponsoring the Article Publication Charge.

References

[1] World Health Organisation (2021) World Malaria Report, Geneva, Switzerland, 2021

[2]. World Health Organisation (2022) Global Malaria Programme, Vector Alert: Anopheles stephensi Invasion and Spread in Africa and Sri Lanka, World Malaria Report, Geneva, Switzerland, 1-4, 978-92-4-0067714.

[3] Ying L, Ragone D, Murch SJ. Breadfruit (*Artocarpusaltilis*): A source of some high-quality protein for food security and novel food products. Amino Acids 2015;47(4):847-856. https://doi.org/10.1007/s00726-015-1914-4.

[4] Jagtap UB and Bapat VA. *Artocarpus*: A Review of its Traditional Uses, Phytochemistry and Pharmacology. J Ethnopharmacol. 2010;129(2):142-66. https://doi.org/10.1016/j.jep.2010.03.031.

[5] Nwokocha C, Palacios J, Simirgiotis MJ. Aqueous extract from leaf of *Artocarpusaltilis* provides cardio-protection from isoproterenol-induced myocardial damage in rats: Negative chronotropic and inotropic effects. J Ethnopharmacol. 2017;203:163-170. https://doi.org/10.1016/j.jep.2017.03.037.

[6] Thomas J, Anderson T, Green TJ. *Artocarpusaltilis* (breadfruit) could reverse myocardial infarction through the normalization of the oxygen haemoglobin dissociation curve. Cardiovasc Hematol Agents Med Chem. 2022. https://doi.org/10.2174/1871525720666220203110919.

[7] Nwokocha CR, Owu DU, McLaren M. Possible mechanisms of action of the aqueous extract of *Artocarpusaltilis* (breadfruit) leaves in producing hypotension in normotensive

Sprague-Dawley rats. Pharm Biol. 2012;50(9):1096-102. https://doi.org/10.3109/13880209.2012.658113.

[8] Ahmad MN, Karim NU, Normaya E. *Artocarpusaltilis* extracts as a food-borne pathogen and oxidation inhibitors: RSM, COSMO RS, and molecular docking approaches. Sci Rep. 2020;10(1):9566. https://doi.org/10.1038/s41598-020-66488-7.

[9] Jalal TK, Ahmed IA, Mikail M. Evaluation of antioxidant, total phenol and flavonoid content and antimicrobial activities of *Artocarpusaltilis* (breadfruit) of underutilized tropical fruit extracts. Appl Biochem Biotechnol. 2015;175(7):3231-43. https://doi.org/10.1007/s12010-015-1499-0.

[10] Soifoini T, Donno D, Jeannoda V. Phytochemical composition, antibacterial activity, and antioxidant properties of the *Artocarpus altilis* fruits to promote their consumption in the Comoros Islands as potential health-promoting food or a source of bioactive molecules for the food industry. Foods 2021;10(9):2136. https://doi.org/10.3390/foods10092136.

[11] Tiraravesit N, Yakaew S, Rukchay R. *Artocarpusaltilis* heartwood extract protects skin against UVB in vitro and *invivo*. J Ethnopharmacol. 2015;175:153-162. https://doi.org/10.1016/j.jep.2015.09.023.

[12] Nguyen MT, Nguyen NT, Nguyen KD. Geranyl dihydrochalcones from *Artocarpusaltilis* and their antiausteric activity. Planta Med. 2014;80(2-3):193-200. https://doi.org/10.1055/s-0033-1360181.

[13] Wang Y, Deng T, Lin L. Bioassay-guided isolation of antiatherosclerotic phytochemicals from *Artocarpusaltilis*. Phytother Res. 2006;20(12):1052-5. https://doi.org/10.1002/ptr.1990.

[14] Suhartati T, Achmad SA, Aimi N. Artoindonesianin L, a new prenylated flavone with cytotoxic activity from *Artocarpusrotunda*. Fitoterapia 2001;72(8):912-8. https://doi.org/10.1016/s0367-326x(01)00343-4.

[15] Shamaun SS, Rahmani M, Hashim NM. Prenylated flavones from *Artocarpusaltilis*. J Nat Med. 2010;64(4):478-81. https://doi.org/10.1007/s11418-010-0427-4.

[16] Hakim EH, Achmad SA, Juliawaty LD. Prenylated flavonoids and related compounds of the Indonesian *Artocarpus* (Moraceae). J Nat Med. 2006;60(3):161-184. https://doi.org/10.1007/s11418-006-0048-0.

[17] Ogundele SB, Oriola AO, Oyedeji AO, Olorunmola FO, Agbedahunsi JM. Flavonoids from Stem Bark of *Artocarpusaltilis* (Parkinson ex F.A. Zorn) Fosberg *Chem Afr* 2022;1-15, https://doi.org/10.1007/s42250-022-00489-z

[18] World Flora Online (WFO). *Artocarpusaltilis*. Published on the Internet; http://www.worldfloraonline.org/taxon/wfo-000050425. Accessed on 6th January, 2022.

[19] Organisation of Economic Cooperation and Developments (OECD) guidelines for Testing Chemicals: Guidelines 425: Acute Oral Toxicity, 2008, Paris, France

[20] Imran IZ, Elusiyan CA, Agbedahunsi JM, Omisore NO. Bioactivity-directed Evaluation of fruit of Kigelia africana (Lam.) Benth. used in the treatment of Malaria Iwo, Nigeria. Journal of Ethnopharmacol., 2021; 268:113680, https://doi.org/10.1016/j.jep.2020.113680

[21] Peters W. Drug Resistance in *Plasmodiumberghei*, Experimental parasitology, 1965; 17:80-89

[22] Ryley J. and Peters W. The Antimalarial Activity of some Quinoline Esters. Annals of Tropical Medicine and Parasitology, 1970; 84:209-222

[23] Sanner MF. Python: a programming language for software integration and development. J Mol Graph Model. 1999 Feb 1;17(1):57-61. doi:

[24] Eberhardt J, Santos-Martins D, Tillack AF, Forli S. AutoDock Vina 1.2. 0: New docking methods, expanded force field, and python bindings. Journal of chemical information and modeling. 2021 Jul 19;61(8):3891-8. doi: 10.1021/acs.jcim.1c00203

[25] Trott O, Olson AJ. Software news and update AutoDock Vina: Improving the speed and accuracy of docking with a new scoring function. Effic. Optim. Multithreading. 2009;31:455-61. doi: 10.1002/jcc.21334

[26] Shah H and Khan AA. Phytochemical characterisation of an important medicinal plant, Chenopodium ambrosioides Linn. Nat Prod Res. 2017;31(19):2321-2324. https://doi.org/10.1080/14786419.2017.1299722.

[27] Hidayathulla S, Shabat AA, Ahamad SR. GC/MS Analysis and characterization of 2-hexadecen-1-ol and beta Sitosterol from *Schimperaarabica* extract for its bioactive potentials as antioxidant and antimicrobial. J Appl Microbiol.(2018);124(5):1082-1091. https://doi.org/10.1111/jam.13704.

[28] Krettli AU, Adebayo O. and Krettli L. G. Testing of Natural Products and Synthetic Molecules aiming at New Antimalarials. Current Drug Targets (2009);10(3):261-270

[29] Adebajo AC, Odediran SA, Aliyu FA, Nwafor PA, Nwoko NT, Umana US. In vivo antiplasmodial potentials of the combinations of four nigerian antimalarial plants. Molecules. (2014);19(9):13136-46. doi: 10.3390/molecules190913136.

[30] Aladesanmi, Joseph A, Odiba, Emmanuel O, Odediran, Akintunde S, Oriola, Olubunmi A. Antiplasmodial Activities of the Stem Bark Extract of *Artocarpus altilis* Forsberg. Afr J Infect Dis. (2022);16(2 Suppl):33-45. doi: 10.21010/Ajid.v16i2S.5.

[31] Hidayati AR, Melinda, Ilmi H, Sakura T, Sakaguchi M, Ohmori J, Hartuti ED, Tumewu L, Inaoka DK, Tanjung M, Yoshida E, Tokumasu F, Kita K, Mori M, Dobashi K, Nozaki T, Syafruddin D, Hafid AF, Waluyo D, Widyawaruyanti A. Effect of geranylated dihydrochalcone from *Artocarpus altilis* leaves extract on *Plasmodium falciparum* ultrastructural changes and mitochondrial malate: Quinone oxidoreductase. Int J Parasitol Drugs Drug Resist. (2022);21:40-50. doi: 10.1016/j.ijpddr.2022.12.001.